Available online at www.sciencedirect.com
SCIENCE DIRECT®
International Journal of Thermal Sciences 42 (2003) 621–630
International Journal of Thermal Sciences
www.elsevier.com/locate/ijts

On Cauchy conditions for asymmetric mixed convection boundary layer flows

Conditions de Cauchy pour une couche limite de convection mixte asymétrique

Mustapha Amaouche [a], Mohand Kessal [b,*]

[a] *Laboratoire de physique théorique, Université de Bejaia, Algérie*
[b] *Département transport et equipement pétrolier, faculté des hydrocarbures et de la chimie, Université de Boumerdes, Boumerdes 35000, Algérie*

Received 26 September 2001; accepted 31 August 2002

Abstract

The fundamental question of how and where does an asymmetric mixed convection boundary layer flow around a heated horizontal circular cylinder begin to develop is raised. We first transform the classical boundary layer equations by using an integral method of Karman–Pohlhausen type and obtain two coupled equations governing the evolutions of the dynamic and thermal boundary layers. Because of its global character, the implemented method allows to bypass the difficulty of downstream–upstream interactions. Cauchy conditions characterizing the starting of the boundary layers are found; they are obtained in a surprisingly simple manner for the limiting cases corresponding to $Pr = 1$, $Pr \to 0$ and $Pr \to \infty$. Otherwise, these conditions can be found by using a prediction correction algorithm. Some numerical experiments are finally performed in order to illustrate the theory.

Résumé

Le problème fondamental du démarrage d'un écoulement de convection mixte asymétrique est posé en termes d'évolution des épaisseurs des couches limites dynamique et thermique. Cette procédure permet, de part son caractère global, d'aplanir les difficultés liées aux interactions amont-aval dues à l'existence d'un écoulement de retour dans la zone de convection mixte défavorable. Les positions des points de départ des couches limites et les conditions de Cauchy correspondantes sont discutées en fonction de la valeur du nombre de Prandtl. Quelques résultats numériques sont présentés afin d'illustrer la présente théorie.

Keywords: Mixed convection; Laminar boundary layer; Asymmetric flow; Circular cylinder; Cauchy conditions

Mots-clés : Convection mixte ; Couche limite laminaire ; Écoulement asymétrique ; Cylindre circulaire ; Conditions de Cauchy

1. Introduction

Mixed convection flow is usually associated with the interaction between forced and free convection acting to either reinforce or oppose one another; it is known since the work by Merkin [1] that, when buoyancy aids motion, separation is delayed, indeed suppressed. In the opposite case the separation point approaches the forward stagnation point by increasing the buoyancy effects and the boundary layer character may be removed beyond certain critical conditions.

When these two effects are uniformly favourable or uniformly unfavourable along the heated body, the boundary layer flow begins from a stagnation point, the location of which and the associate Cauchy conditions may be deduced by using the symmetry properties of the flow. For instance, in the case of a horizontal cylinder, the flow is symmetric about a vertical plane containing the axis of the cylinder if

* Corresponding author.
E-mail addresses: m_amaouche@yahoo.fr (M. Amaouche), m.kessal@voila.fr (M. Kessal).

1290-0729/03/$ – see front matter
doi:10.1016/S1290-0729(03)00027-9

Nomenclature

a	cylinder radius ..... m
g	gravity acceleration ..... $m{\cdot}s^{-2}$
Gr	Grashof number
Jx	tangential component of the upward unit vector
Nu	Nusselt number
Pr	Prandtl number
Re	Reynolds number
Ri	Richardson number
T	dimensional temperature ..... K
u_e	potential velocity field
u, v	angular and normal velocity components
u_∞	dimensional free stream velocity ..... $m{\cdot}s^{-1}$
x, y	angular and normal coordinates

Greek symbols

α	inclination of the free stream from the vertical ..... rd
β	coefficient of thermal expansion ..... K^{-1}
δ_d	dimensionless dynamic boundary layer thickness
δ_T	dimensionless thermal boundary layer thickness
Δ	$= \delta_T/\delta_d$
δ	$= \delta_d^2$
θ	normalized temperature
ν	kinematic viscosity ..... $m^2{\cdot}s^{-1}$
ζ	$= y/\delta_d$
η	$= y/\delta_T$
$\tilde{\Lambda}$	mixed convection function
τ_w	wall skin friction

Subscripts

e	potential flow
s	separation point
w	heated surface
∞	free stream
0	starting point
x, y	partial derivation with respect to x, y

the constant far stream is vertical and the stagnation point is either the lowest or the upper most point of the cylinder, depending on the particular data of the problem. Near the stagnation point, the flow is described by a self similar solution which constitutes the first term of a Blasius series; the higher order terms are then obtained recursively from the first one [2].

The Blasius procedure fails to be valid in certain circumstances as in the case when the free stream is nonvertically directed [3]. This failure expresses the loss of Cauchy conditions for the boundary layer evolution and is a result of the coexistence and the alternation of favourable and opposite mixed convection domains. The location of the stagnation point is not known and is somewhere in the unfavourable mixed convection domain, between the lowest point of the heated cylinder and the stagnation point of the potential flow. In this region, the boundary layer is composed of an inflow part near the wall, driven primarily by buoyancy, and an outflow part driven by the external boundary condition. Therefore, this particular structure of the boundary layer flow resembles that which occurs in the reattachment region because buoyancy behaves like an increasing adverse pressure gradient. The situation is also similar to that encountered near a separation point where the boundary layer equations for two-dimensional incompressible fluid flow possess a singularity when an outer pressure distribution is prescribed. In practice, the latter is locally altered near the separation point in a manner which allows the boundary layer solution to be regular. By requiring the displacement thickness to assume a non-singular form, Catherall and Mangler [4] have numerically integrated the boundary layer equations beyond the separation point and obtained regular solutions with a reverse flow. The unknown pressure distribution was then calculated as a part of the numerical integration procedure. However, the occurrence of reverse flow introduces a mechanism of influence of the downstream conditions on the evolution of the boundary layer. This behaviour which is consistent with the elliptic nature of the Navier–Stokes equations is also authorized by using another boundary condition for closure. One of the recent study in this area is realized by Higuera [5] who solved numerically the problem for mixed convection in a wall jet over a finite length horizontal plate by taking into account the upstream information propagation due to the buoyancy induced pressure. In spite of the great number of available studies in this area, we are not aware of any work on mixed convection flows where the question of the stagnation point location and the corresponding Cauchy conditions is posed for an asymmetric boundary layer. This question is fundamental because it would enable us to understand where and how the boundary layer begins to develop and therefore to determine its evolution along the heated body.

It is the purpose of this paper to seek the location of the stagnation point which results from the local equilibrium between forced and free convection effects and to carry out a local analysis in order to characterize the starting of the boundary layer flow. This will be achieved by using an approximate method of Karman–Pohlhausen type. The result suggests that the global character of the approximation may overcome the difficulty arising from the upstream-downstream interaction and allows to recover, in the mean sense, the parabolic nature of the problem.

This paper is organized as follows. In the following section we will briefly list the basic equations. We will

continue with the description of the integral formulation in Section 3. This section will also give the coupled evolution equations for the boundary layer thicknesses. The Cauchy conditions for these equations will be discussed in Section 4. Then some numerical results will be given. Finally we will present our concluding remarks and indicate suggestions for further work.

2. Basic equations

We consider a two-dimensional steady and laminar boundary layer flow around a heated horizontal circular cylinder, under the combined effects of forced and free convection. The cylinder is placed in a nonvertically oriented free stream. Let α be the inclination of the latter with respect to the vertical. One can expect that same qualitative behaviours occur at the stagnation point flow whatever α in the range $(0, \pi)$. So it suffices, in order to illustrate the purpose, to restrict ourselves to the intermediate case $\alpha = \pi/2$ (the schematic of the problem is given in Fig. 1). By using the classical Boussinesq approximation, the governing equations and boundary conditions may be written in dimensionless form as:

$$u_x + v_y = 0 \tag{2.1}$$

$$uu_x + vu_y = u_e \frac{\mathrm{d}u_e}{\mathrm{d}x} + Ri\,Jx\theta + u_{yy} \tag{2.2}$$

$$Pr(u\theta_x + v\theta_y) = \theta_{yy} \tag{2.3}$$

$$\left.\begin{array}{l} u = v = 0 \quad \theta = 1 \quad \text{on } y = 0 \\ u \to u_e(x) \quad \theta \to 0 \quad \text{as } y \to \infty \end{array}\right\} \tag{2.4}$$

In these equations, the radius a of the cylinder is chosen as a lengthscale for the nondimensionalization of the azimuthal coordinate x whose origin is at the stagnation point of the potential flow. The radial coordinate y, counted from the wall, is rendered dimensionless by the scale factor $a\,Re^{-1/2}$ in order that y be of order unity in the boundary layer; Re denotes the Reynolds number $u_\infty a/\nu$ where u_∞ designates the constant free stream velocity and ν the kinematic viscosity. The angular and radial velocity components u and v are scaled by u_∞ and $u_\infty Re^{-1/2}$, respectively. The functions u_e $(= 2\sin x)$ and Jx $(= \sin(x + \alpha))$ indicate the dimensionless external flow velocity alongside the cylinder and the tangential component of the upward unit vector. The normalized temperature θ is related to the dimensional temperature T by $\theta = (T - T_\infty)/(T_w - T_\infty)$ where T_w and T_∞ stand for the (constant) wall and ambient temperatures, respectively. Finally Pr and Ri are, respectively, the Prandtl number and the Richardson number $(Gr\,Re^{-2})$, Gr being the Grashof number $(g\beta(T_w - T_\infty)a^3/\nu^2)$ where g is the gravitational acceleration and β the thermal expansion coefficient.

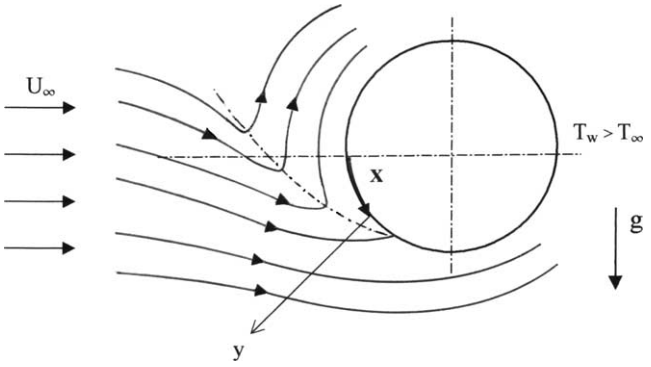

Fig. 1. Schematic of the flow.

In order that the parabolic problem (2.1)–(2.4) be well posed, it must be completed by the appropriate Cauchy conditions on the evolutionary variable x. This question will be examined in Section 4.

3. Evolution equations for boundary layer thicknesses

First of all, we introduce two similarity variables, namely $\zeta = y/\delta_d(x)$ and $\eta = y/\delta_T(x)$ where $\delta_d(x)$ and $\delta_T(x)$ are the local dynamic and thermal boundary layer thicknesses, respectively. After this we look for an approximate solution by representing the velocity and temperature profiles by fourth order polynomials in ζ and η. Taking into account the outer matching conditions and the conditions at $y = 0$, we obtain:

$$u(x, y) = u_e(x)\big\{1 - F(\zeta)\big\} + \tilde{\Lambda}(x)G(\zeta) \tag{3.1}$$

$$\theta(x, y) = F(\eta) \tag{3.2}$$

where:

$$\begin{aligned} &F(\zeta) = (1 - \zeta)^3(1 + \zeta), \\ &G(\zeta) = \frac{1}{6}\zeta(1 - \zeta)^3 \end{aligned} \tag{3.3}$$

$$\tilde{\Lambda}(x) = \delta_d^2(x)\left(u_e \frac{\mathrm{d}u_e}{\mathrm{d}x} + Ri\,Jx\right) \equiv \delta_d^2(x) f(x) \tag{3.4}$$

It is to be noted that the approximations (3.1) and (3.2) remain incomplete because they are subordinated to the knowledge of $\delta_d(x)$ and $\delta_T(x)$. The equations governing the evolution of δ_d and δ_T are obtained by integrating the momentum and energy equations along the radial direction and over δ_d and δ_T, respectively. To avoid duplication of elementary steps, we only give the results in the form:

$$\frac{\mathrm{d}\tilde{\delta}_2}{\mathrm{d}x} + \tilde{\delta}_1 \frac{\mathrm{d}u_e}{\mathrm{d}x} = \tau_w - Ri\,Jx\,I_d \tag{3.5}$$

$$Pr \frac{\mathrm{d}I_T}{\mathrm{d}x} = Nu \tag{3.6}$$

where the notations are as follows:

$$\tau_w = \left.\frac{\partial u}{\partial y}\right|_{y=0}$$

is the wall shear stress and

$$Nu = -\left.\frac{\partial \theta}{\partial y}\right|_{y=0}$$

is the Nusselt number.

$$\left.\begin{aligned} I_d &= \int_0^{\delta_d} \theta(x,y)\,\mathrm{d}y, \qquad I_T = \int_0^{\delta_T} u\theta(x,y)\,\mathrm{d}y \\ \tilde{\delta}_1 &= \int_0^{\delta_d} (u_e-u)\,\mathrm{d}y, \qquad \tilde{\delta}_2 = \int_0^{\delta_d} u(u_e-u)\,\mathrm{d}y \end{aligned}\right\} \tag{3.7}$$

For their regularity, the two last quantities are preferred to the classical displacement and momentum thicknesses which are singular at the stagnation point of the potential flow. This singularity is removed only in certain special configurations among which is the symmetric case. Introducing expressions (3.1) and (3.2) for u and θ into integrals (3.7) gives:

$$\tilde{\delta}_1 = \delta_d\left(\frac{3}{10}u_e - \frac{1}{120}\tilde{\Lambda}\right) \equiv P_1\big(u_e,\tilde{\Lambda}\big)\delta_d \tag{3.8}$$

$$\begin{aligned} \tilde{\delta}_2 &= \delta_d\left(\frac{37}{315}u_e^2 - \frac{1}{945}u_e\tilde{\Lambda} - \frac{1}{9072}\tilde{\Lambda}^2\right) \\ &\equiv P_2\big(u_e,\tilde{\Lambda}\big)\delta_d \end{aligned} \tag{3.9}$$

$$I_d = \delta_d H_0(\Delta)$$

$$I_t = \delta_d\big(u_e H_1(\Delta) + \tilde{\Lambda} H_2(\Delta)\big)$$

where Δ denotes the ratio δ_T/δ_d and the functions H_0, H_1 and H_2 are (see Appendix A):

$$\left.\begin{aligned} H_0 &= \frac{3}{10}\Delta \\ H_1 &= \Delta^2\left(\frac{2}{15} - \frac{3}{140}\Delta^2 + \frac{1}{180}\Delta^3\right) \\ H_2 &= \Delta^2\left(\frac{1}{90} - \frac{1}{84}\Delta + \frac{3}{560}\Delta^2 - \frac{1}{1080}\Delta^3\right) \end{aligned}\right\} \tag{3.10}$$

for $\Delta \leqslant 1$ $(Pr \geqslant 1)$

$$\left.\begin{aligned} H_0 &= 1 - \Delta^{-1} + \frac{1}{2}\Delta^{-3} - \frac{1}{5}\Delta^{-4} \\ H_1 &= \frac{3}{10}\Delta - \frac{3}{10} + \frac{2}{15}\Delta^{-1} - \frac{3}{140}\Delta^{-3} + \frac{1}{180}\Delta^{-4} \\ H_2 &= \frac{1}{120} - \frac{1}{180}\Delta^{-1} + \frac{1}{840}\Delta^{-3} - \frac{1}{3024}\Delta^{-4} \end{aligned}\right\} \tag{3.11}$$

for $\Delta \geqslant 1$ $(Pr \leqslant 1)$

Finally the wall shear stress and the Nusselt number are expressed as follow:

$$\left.\begin{aligned} \tau_w &= \frac{(2u_e + \tilde{\Lambda}/6)}{\delta_d} \equiv \frac{P_0(u_e,\tilde{\Lambda})}{\delta_d} \\ Nu &= \frac{2}{\delta_d \Delta} \end{aligned}\right\} \tag{3.12}$$

We can now transform Eqs. (3.5) and (3.6) by means of relations (3.8)–(3.12) into two coupled evolution equations for δ (the square of δ_d) and Δ, namely:

$$P\frac{\mathrm{d}\delta}{\mathrm{d}x} = S \tag{3.13}$$

$$Q\frac{\mathrm{d}\delta}{\mathrm{d}x} + R\frac{\mathrm{d}\Delta}{\mathrm{d}x} = K \tag{3.14}$$

with:

$$\left.\begin{aligned} P &= P_2 + 2\tilde{\Lambda}\frac{\partial P_2}{\partial \tilde{\Lambda}} \\ S &= 2\left[P_0 - \frac{\partial P_2}{\partial \tilde{\Lambda}}\frac{\mathrm{d}f}{\mathrm{d}x}\delta^2 \right. \\ &\qquad \left. - \delta\left(Ri\,Jx\,H_0 + \frac{\mathrm{d}u_e}{\mathrm{d}x}\left(P_1 + \frac{\partial P_2}{\partial u_e}\right)\right)\right] \end{aligned}\right\} \tag{3.15}$$

$$\left.\begin{aligned} Q &= \frac{\Delta}{2}\big(u_e H_1 + 3\tilde{\Lambda} H_2\big) \\ R &= \Delta\delta\left(u_e\frac{\mathrm{d}H_1}{\mathrm{d}\Delta} + \tilde{\Lambda}\frac{\mathrm{d}H_2}{\mathrm{d}\Delta}\right) \\ K &= \frac{2}{Pr} - \Delta\delta\left(H_1\frac{\mathrm{d}u_e}{\mathrm{d}x} + \delta H_2\frac{\mathrm{d}f}{\mathrm{d}x}\right) \end{aligned}\right\} \tag{3.16}$$

4. Cauchy conditions

In order to set up a closed problem, the dynamic system (3.13), (3.14) must be completed by appropriate Cauchy conditions. These are obtained by assuming regular behaviours for the fundamental variables δ and Δ. This is possible only under certain reserves depending on whether the problem is symmetric or not.

4.1. Symmetric case

Let us recall that the symmetric problem is characterized by a vertically oriented free stream. In this configuration, the stagnation point is known in advance and is naturally the forward stagnation point of the potential flow. At this point, we have of course:

$$(P, Q, R) = (0, 0, 0) \tag{4.1}$$

since $u_e(0) = Jx(0) = 0$ and therefore $\tilde{\Lambda}(0) = 0$. Hence, one may write:

$$\frac{S}{u_e}(Ri, \delta, \Delta, x = 0) = 0 \tag{4.2}$$

$$K(Ri, Pr, \delta, \Delta, x = 0) = 0 \tag{4.3}$$

These equations are coupled via the term $H_0(\Delta)$. Their resolution provides the values δ_0 and Δ_0 at $x = 0$ as functions of Ri depending on the parameter Pr. Moreover, one may conclude again that

$$\left(\frac{\mathrm{d}\delta}{\mathrm{d}x}\right)_{x=0} = \left(\frac{\mathrm{d}\Delta}{\mathrm{d}x}\right)_{x=0} = 0$$

since Eqs. (2.1)–(2.4) remain unchanged by the transformation

$$(x, y, u, v, \theta) = (-x, y, -u, v, \theta) \tag{4.4}$$

This invariance comes from the symmetry property of $u_e(x)$ and hence of $Jx(x)$.

4.2. Asymmetric case

In the asymmetric case, the free stream is not vertically oriented, so the external velocity field and the tangential component of the buoyancy force are described by two different functions. As a result, the invariance property discussed above is no longer satisfied. Then, neither $x = 0$, nor the abscissa of the lowest point of the cylinder does constitute a solution for Eq. (4.1). One can however expect that the location of the point where the boundary layer begins to develop is somewhere in the unfavourable mixed convection region, between the stagnation points of free and forced convection. Owing to the parabolic nature of the problem in the symmetric case and because of the reversal direction of the flow in the present case, the procedures which are used to describe the beginning of the boundary layer in each of them are slightly different. In the asymmetric case the Prandtl number which characterizes the importance of thermal convection plays the leading part in the procedure. For convenience, but without loss of generality, we consider, as it is mentioned previously, only the case $\alpha = \pi/2$.

4.2.1. Pr is close to unity

When the Prandtl number is of order unity, the two boundary layers are of the same size, so the ratio Δ is of order unity. Hence, Eq. (3.13) suffices to describe the communal thickness of the two layers. In order that $x \to \delta(x)$ be a smooth function, the existence of a particular station x_0 where $P(x_0) = 0$ requires that at this station S must also vanish. One can readily find that where the second order polynomial $P(u_e, \tilde{\Lambda})$ vanishes, one must have either

$$\tilde{\Lambda} = 12u_e \tag{4.5}$$

or

$$\tilde{\Lambda} = -17.76u_e \tag{4.6}$$

The first condition is not realistic because it does not allow to recover the results of the limiting case of forced convection by taking the limit $Ri \to 0$.

The second condition which will be considered later, yields a realistic description of the boundary layer flow, including particular configurations such as forced, free and symmetric mixed convection. The next step consists of seeking the location of the starting point of the boundary layer. Using the relation (4.6) with the definition (3.4), the condition $S = 0$ is transformed into a single variable equation whose solution gives the starting point x_0. This value of course depends on the mixed convection parameter Ri. The value δ_0 of δ at $x = x_0$ is then deduced from (3.4) with the aid of (4.6).

Because of the vanishing of both P and S at $x = x_0$, the derivative $(\frac{d\delta}{dx})_{x_0}$ must be determined to complete the formulation of the initial value problem. Making use of the Taylor expansion and keeping only the first order terms, the following second order algebraic equation is obtained for $(\frac{d\delta}{dx})_{x_0}$

$$A_0\left(\frac{d\delta}{dx}\right)_{x_0}^2 + 2B_0\left(\frac{d\delta}{dx}\right)_{x_0} + C_0 = 0 \tag{4.7}$$

The coefficients A_0, B_0 and C_0 are given in Appendix B.

4.2.2. $Pr \to 0$

We first note that if Pr is much less then unity, heat is transferred mainly by conduction and therefore δ_T becomes infinitely large, whilst δ remains a well-defined function, so $\Delta \to \infty$ and H_0, H_1 and H_2 take the asymptotic following forms

$$H_0 \cong 1, \qquad H_1 \cong \frac{3}{10}\Delta, \qquad H_2 \cong \frac{1}{120} \tag{4.8}$$

The approximation $H_0 = 1$ yields the decoupling of the evolutions of the two boundary layers since Eq. (3.13) is no longer dependent on Δ. Furthermore, this equation becomes then similar to that corresponding to the case $Pr = 1$ with a simple modification of the global buoyancy term.

The evolution of Δ which is slaved to that of δ starts from the stagnation point of the potential flow ($x = 0$) because R is here proportional to $u_e(x)$ and therefore $R(x = 0) = 0$. Accordingly, Eq. (3.14) yields:

$$\left(K - Q\frac{d\delta}{dx}\right)_{x=0} = 0 \tag{4.9}$$

which can be written in accordance to (3.13)

$$(PK - QS)_{x=0} = 0 \tag{4.10}$$

solving this equation gives an approximate value of δ_T at $x = 0$ in the form:

$$\delta_T \approx \left(\frac{3}{10}Pr\right)^{-1/2} \tag{4.11}$$

This formula shows that in the limit $Pr \to 0$, the thermal boundary layer thickness at the stagnation point of the potential flow is determined only by the Prandlt number.

4.2.3. $Pr \to \infty$

In the limit of large Prandtl numbers, we recall that heat is rather convected by the fluid flow except in a very thin thermal boundary layer. Since the thickness δ_T and the ratio Δ become vanishingly small then the functions H_0, H_1 and H_2 may be asymptotically approached by:

$$H_0 \cong 0, \qquad H_1 \cong \frac{2}{15}\Delta^2, \qquad H_2 \cong \frac{1}{90}\Delta^2 \tag{4.12}$$

As in the previous case the thermal boundary layer evolution follows that of the dynamic boundary layer because $H_0 = 0$ and therefore the right-hand side of (3.13) does not either depend on Δ. For this reason, Eq. (3.13) appears as a forced convection equation where buoyancy terms are implicitly taken into account via the mixed convection function $\tilde{\Lambda}(x)$. The procedure used in the case $Pr = 1$ is also applied to seek the station where the dynamic boundary layer begins

to develop. Concerning the evolution of the thermal boundary layer, it is advisable to firstly note that, in view of (4.10), the function R takes the form:

$$R \approx \frac{1}{45}\delta_T^2\left(\tilde{\Lambda} + 12u_e\right) \tag{4.13}$$

It becomes zero at the station x_0^* where $\tilde{\Lambda} = -12u_e$, that is precisely where $\tau_w = 0$. This means that the point of zero skin friction marks the beginning of the thermal boundary layer. Here, the value Δ_0 of Δ is found by solving Eq. (4.10) at x_0^*. This equation can again be solved explicitly in view of (4.12), one obtains:

$$\Delta_0 = Pr^{-1/3}\left(\frac{120P}{(\tilde{\Lambda}+4u_e)S + \delta P(8\frac{\mathrm{d}u_e}{\mathrm{d}x} + \frac{2}{3}\delta\frac{\mathrm{d}f}{\mathrm{d}x})}\right)^{1/3}_{x=x_0^*} \tag{4.14}$$

which gives after some elementary steps:

$$(\delta_T)_{x_0^*} = Pr^{-1/3}\left(\frac{30\delta_d}{\frac{\mathrm{d}}{\mathrm{d}x}(\tau_w\delta_d)}\right)^{1/3}_{x=x_0^*} \tag{4.15}$$

This is in agreement with the classical result which tells us that the thermal boundary layer thickness behaves like $Pr^{-1/3}$ as $Pr \to \infty$.

In the present asymptotic case we note that the initial value given by (4.15) depends on the history of the flow from the starting point of the dynamic boundary layer. In order to complete the initial conditions for Eq. (3.14) a Taylor expansion is finally performed to express the value $(\frac{\mathrm{d}\Delta}{\mathrm{d}x})_{x_0^*}$.

4.2.4. The general case of finite values of Pr

The main feature of the previous particular cases is that the dynamic boundary layer evolves independently of the thermal one. Its evolution is however influenced by buoyancy. Once the dynamic boundary layer is determined for all x, the equation governing the evolution of Δ is then integrated. For an arbitrary value of Pr, the two boundary layers interact, so the coupled Eqs. (3.13) and (3.14) must be solved simultaneously. Furthermore, this case is of particular relevance because the conditions required to start the integration are no longer available. In order to circumvent this last difficulty, a prediction–correction iterative procedure is implemented and the missing conditions are sought by proceeding as follow. We gradually increase or decrease the value of Pr from the limiting values $Pr \to 0$, $Pr \to 1$ and $Pr \to \infty$ for which the solutions are already known. For a given value of Pr, an estimate of Δ, say Δ_0, is required to initialize the procedure. To this end, the solution corresponding to a previous value of Pr is chosen. Proceeding as before, the couple (x_0, δ_0) is then calculated. Performing a first order Taylor expansion of (3.13) near x_0 and making use of (3.14) to eliminate $(\frac{\mathrm{d}\Delta}{\mathrm{d}x})_{x_0}$, we get an equation similar to (4.7) which allows to express $(\frac{\mathrm{d}\delta}{\mathrm{d}x})_{x_0}$.

Subject to these predicted conditions, Eqs. (3.13) and (3.14) can be numerically solved by using a fourth order Runge–Kutta scheme. In order to the evolutions of δ and Δ be realistic, the factor R and the expression $(PK - QS)$ must cancel at the same station, say x_1. Otherwise, the predicted value Δ_0 is corrected and the procedure is repeated until convergence is reached.

5. Some numerical results

Information about the influence of Prandtl number on the variation of the dynamic boundary layer thickness at the stagnation point with Ri can be gained from Fig. 2(a) ($Pr \leqslant 1$) and (b) ($Pr \geqslant 1$). First of all, it is not surprising that the curves all converge to a same point in the forced convection regime. Fig. 2(a) indicates that the boundary layer thickness at $x = 0$ is a smoothly decreasing function with respect to Ri for the reference case $Pr = 1$ and for Pr less than unity. It appears that the rate of decrease is more important for small Pr. We also observe the breakdown of boundary layer character, in the opposite mixed convection, beyond some critical value of $|Ri|$ which decreases by decreasing Pr. Qualitatively opposite observations can be made from Fig. 2(b), concerning the effects of moderate and large values of Pr. Here, the boundary layer is removed, for assisting external flow, if the Richardson number exceeds some threshold value which is closed to 0.1 as $Pr \to \infty$. The increasing departure with $|Ri|$ from the base case $Pr = 1$ is an indication of the importance of the Prandtl number on the convective properties of the flow.

To illustrate how the buoyancy force and the Prandtl number affect the thermal boundary layer, representative distributions of Δ (rescaled by the factor $Pr^{1/3}$) for $Pr \geqslant 1$ and of δ_T for $Pr \leqslant 1$ are shown in Fig. 2(c) and (d), respectively. The reference case ($Pr = 1$, $\Delta = 1$) is included for comparison. Let us notice that the relation (4.15) corresponding to the asymptotic case $Pr \to \infty$ becomes in the symmetric configuration:

$$Pr^{1/3}(\Delta)_{x=0} = \left[\frac{2}{15}\delta_0 + \frac{1}{180}\delta_0^2(Ri+4)\right]^{-1/3} \tag{5.1}$$

Then, the behaviour of the thermal layer thickness as function of Ri for $Pr \to \infty$ follows from that of the dynamic layer thickness δ_d. We observe a monotonic decrease of Δ for all Pr, in accordance with the evolution given by Polidori et al. [6].

For Pr less than unity, δ_T is preferred to Δ owing to the fact that $\delta_T\, Pr^{1/2}$ behaves like a constant as $Pr \to 0$, in view of (4.11). For this range of Pr, δ_T is lying between the extreme limits corresponding to $Pr = 1$ and to asymptotically small Pr.

In Fig. 2(e) we have displayed the variation of the separation point x_s with Ri in the symmetric case corresponding to opposite ($Ri < 0$) and favourable ($Ri > 0$) mixed convection. After proper implementation of notational changes, results given by Merkin's model for $Pr = 1$ are closely recovered near the forced convection regime. Noticeable divergences

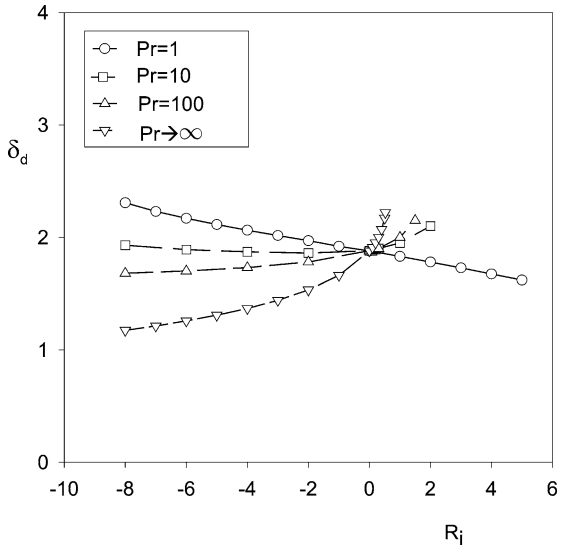

(a)

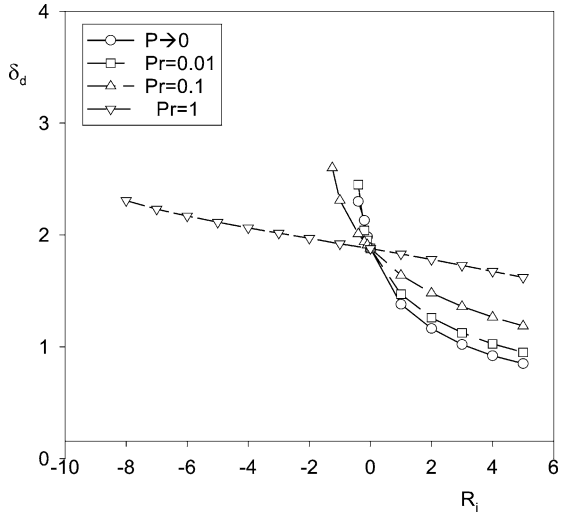

(b)

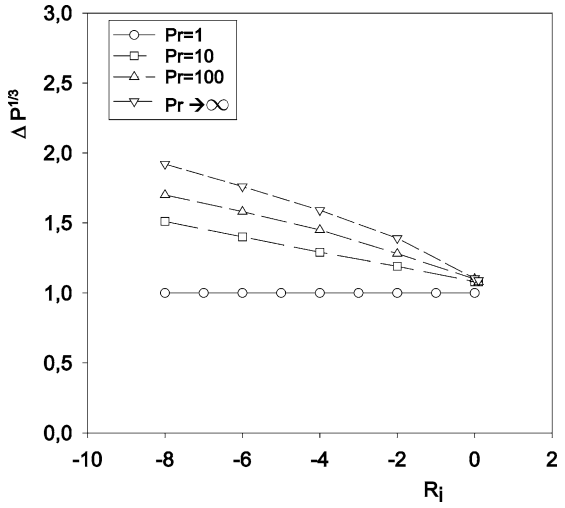

(c)

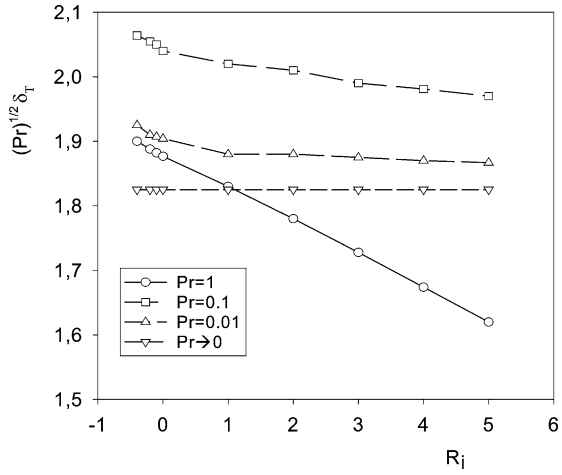

(d)

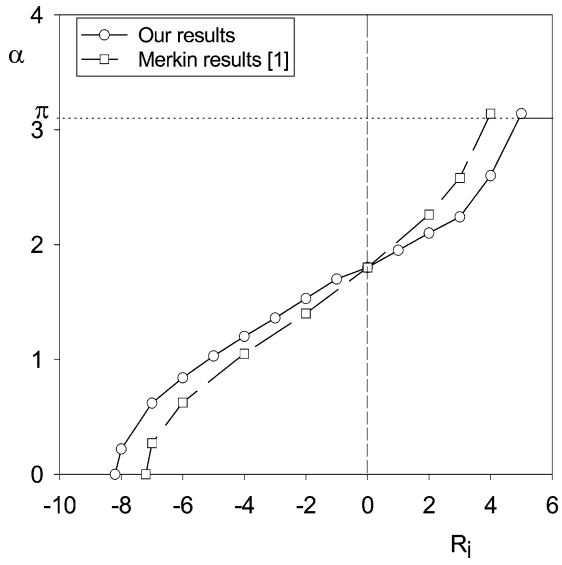

(e)

Fig. 2. Symmetric case: (a) Initial value of δ_d as function of Ri for $Pr \geqslant 1$. (b) Initial value of δ_d as function of Ri for $Pr \leqslant 1$. (c) Initial value of Δ as function of Ri for $Pr \geqslant 1$. (d) Initial value of δ_T as function of Ri for $Pr \leqslant 1$. (e) Variation of the separation point x_s with Ri.

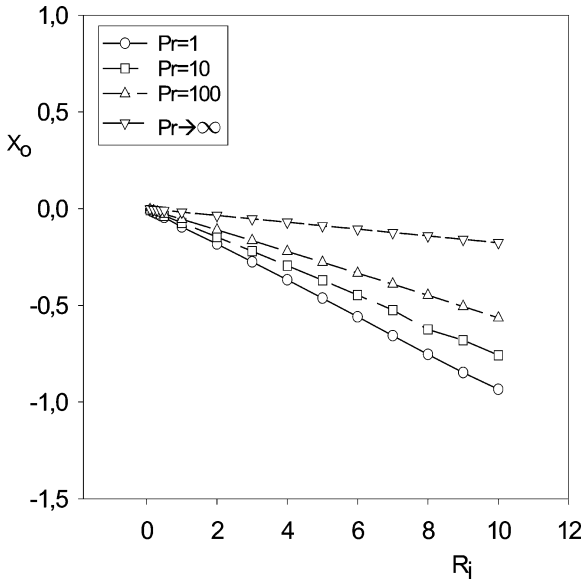

(a)

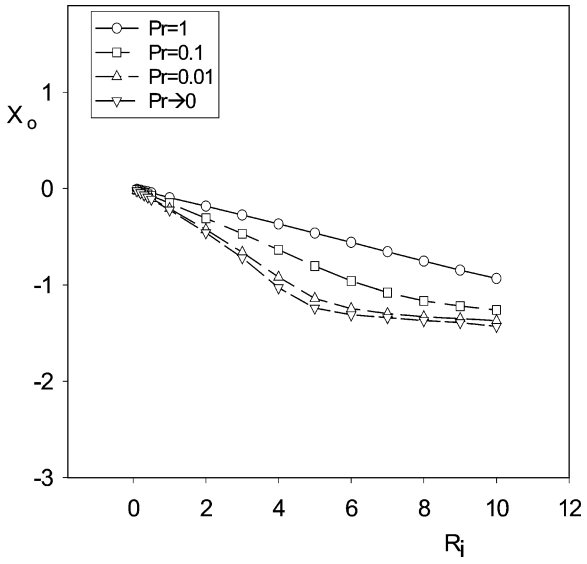

(b)

Fig. 3. Location of the stagnation point versus Ri. (a) For $Pr \geqslant 1$. (b) For $Pr \leqslant 1$.

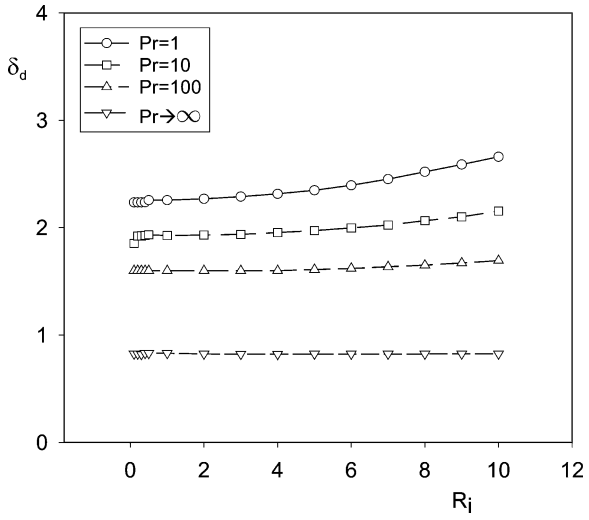

(a)

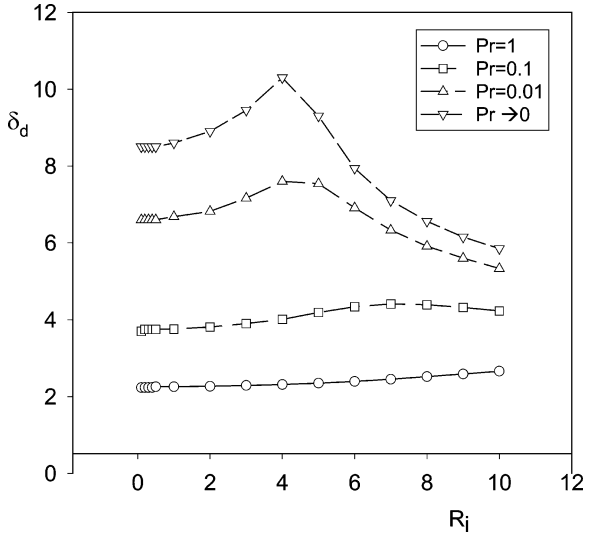

(b)

Fig. 4. Variation of the initial value of δ_d with respect to Ri (asymmetric case): (a) For $Pr \geqslant 1$. (b) For $Pr \leqslant 1$.

appear as $|Ri|$ is increased, especially for positive value of Ri. The critical value of Ri which first gives no separation is difficult to determine as it is noted by Merkin [1]. We do not know how to explain the discrepancies for the computational approaches are very different.

Concerning the asymmetric configuration, only positive values of Ri are considered owing to the symmetry properties of the problem when $\alpha = \pi/2$. Plots of the starting point x_0 of the dynamic boundary layer with respect to Richardson number for the same representative values of Pr are given in Fig. 3(a) and (b). It is to be noted that heating the cylinder brings the point x_0 nearer to the lower point. Increasing Pr makes this tendency less noticeable and for Pr greater than some limit which is of order unity, the shift of the starting point from its positions in forced convection is a nearly linear function of Ri. In the limit $Pr \to 0$, x_0 asymptotes the lower point when Ri is large enough. These results are in accordance with the Prandtl number effects. In the range of Prandtl numbers less than unity, this shift exhibits a change in incline for small Pr and at about $Ri = 4$. Beyond this value of Ri and as $Pr \to 0$, the starting point of the boundary layer approaches closely the lower point. In this situation, the boundary layer flow globally resembles to that of free convection. Fig. 4(a) is a plot of δ_d versus Ri for moderate and large values of Pr. It is seen that, for a fixed Ri, δ_d is a decreasing function of Pr; it grows with Ri especially when Pr is closed to unity. Fig. 4(b) presents a particular interest owing to the seemingly strange behaviour of δ_d with Ri for asymptotically small Pr. We observe indeed a change in incline at certain value of Ri ($Ri = 4$ for $Pr \to 0$). For Ri less than this limit, δ_d grows with Ri

and decreases beyond this limit. The reason for this follows from Fig. 3(b) because when *Ri* is greater than the previous limit, the starting point of the boundary layer approaches closely the lower point where δ_d decreases with *Ri* according to Fig. 2(b).

6. Concluding remarks

The nonexistence of trivial Cauchy conditions for an asymmetric mixed convection problem is the result of the interaction between ascending buoyancy driven flow near the wall and descending flow far away from the wall. This confers to the boundary layer flow an elliptic character. The use of the integral method of Karman–Pohlhausen type allows to characterize the beginning of the boundary layer and therefore to recover the parabolic nature of the flow in the global sense. It is shown that the two boundary layers do not start from the same point except for $Pr = 1$. For this particular value of *Pr*, the starting point is found as root of an algebraic equation, depending on the Richardson number. A similar equation is solved in order to found the location of the starting point and initial conditions for the dynamic boundary layer in the limiting cases of small and large *Pr*. In the former one the thermal boundary begins to develop from the stagnation point of the potential flow. It begins to develop from the point of vanishing skin friction in the second one. For an arbitrary value of *Pr*, a prediction correction procedure is required for solving the problem. It is worth noting that the starting point of the thermal boundary layer is either at the left or at the right of dynamic boundary layer one's, depending on whether *Pr* is smaller than unity or not.

Acknowledgements

The authors are grateful to the referees for their attention to the manuscript and useful comments.

Appendix A

$$I_d = \int_0^{\delta_d} \theta(x, y)\,\mathrm{d}y = \begin{cases} \delta_d \Delta \displaystyle\int_0^1 F(\eta)\,\mathrm{d}\eta & \text{for } \delta_T < \delta_d \\ \delta_d \Delta \displaystyle\int_0^{1/\Delta} F(\eta)\,\mathrm{d}\eta & \text{for } \delta_T > \delta_d \end{cases}$$

In view of (3.3), I_d becomes:

$$I_d = \delta_d H_0(\Delta)$$

$$I_T = \begin{cases} \delta_T \displaystyle\int_0^1 u(\zeta)\theta(\eta)\,\mathrm{d}\zeta & \text{for } \delta_T < \delta_d \\ \displaystyle\int_0^{\delta_d} u\theta\,\mathrm{d}y + \int_{\delta_d}^{\delta_T} u_e\theta\,\mathrm{d}y & \text{for } \delta_T > \delta_d \end{cases}$$

By using (3.1) and (3.2) I_T can be written:

$$I_T = \delta_T \left\{ u_e \int_0^1 \big[1 - F(\zeta)\big] F(\eta)\,\mathrm{d}\eta + \tilde{\Lambda}(x) \int_0^1 G(\zeta) F(\eta)\,\mathrm{d}\eta \right\} \quad \text{for } \Delta < 1$$

and for $\Delta > 1$, we have:

$$I_T = \delta_T \left\{ u_e \int_0^{1/\Delta} \big(1 - F(\zeta)\big) F(\eta)\,\mathrm{d}\eta + \tilde{\Lambda}(x) \int_0^{1/\Delta} G(\zeta) F(\eta)\,\mathrm{d}\eta + u_e \int_{1/\Delta}^{\Delta} F(\eta)\,\mathrm{d}\eta \right\}$$

which can be written as:

$$I_T = \delta_T \left\{ u_e \left(\int_0^1 F(\eta)\,\mathrm{d}\eta - \int_0^{1/\Delta} F(\zeta) F(\eta)\,\mathrm{d}\eta \right) + \tilde{\Lambda}(x) \int_0^{1/\Delta} G(\zeta) F(\eta)\,\mathrm{d}\eta \right\} \quad \text{for } \Delta > 1$$

The formulas (3.16) follow by putting:

$$H_1(\Delta) = \begin{cases} \displaystyle\int_0^1 \big(1 - F(\varsigma)\big) F(\eta)\,\mathrm{d}\eta & \text{for } \Delta < 1 \\ \displaystyle\int_0^1 F(\eta)\,\mathrm{d}\eta - \int_0^{1/\Delta} F(\varsigma) F(\eta)\,\mathrm{d}\eta & \text{for } \Delta > 1 \end{cases}$$

$$H_2(\Delta) = \begin{cases} \displaystyle\int_0^1 G(\varsigma) F(\eta)\,\mathrm{d}\eta & \text{for } \Delta < 1 \\ \displaystyle\int_0^{1/\Delta} G(\varsigma) F(\eta)\,\mathrm{d}\eta & \text{for } \Delta > 1 \end{cases}$$

Appendix B

$$A_0 = f \frac{\partial P_3}{\partial \tilde{\Lambda}}$$

$$B_0 = \frac{\mathrm{d}u_e}{\mathrm{d}x}\left[\frac{\partial P_3}{\partial u_e} + P_5 + \tilde{\Lambda}\frac{\partial P_5}{\partial \tilde{\Lambda}}\right] + \delta\frac{\mathrm{d}f}{\mathrm{d}x}\left[\frac{\partial P_3}{\partial \tilde{\Lambda}} + 2P_4 + \tilde{\Lambda}\frac{\partial P_4}{\partial \tilde{\Lambda}}\right] + \frac{3}{5}Ri\,Jx - 2f\frac{\partial P_0}{\partial \tilde{\Lambda}}$$

$$C_0 = \delta^3\frac{\partial P_4}{\partial \tilde{\Lambda}}\left(\frac{\mathrm{d}f}{\mathrm{d}x}\right)^2 + \delta^2\left[P_4\frac{\mathrm{d}^2 f}{\mathrm{d}x^2} + \frac{\mathrm{d}u_e}{\mathrm{d}x}\frac{\mathrm{d}f}{\mathrm{d}x}\left(\frac{\partial P_5}{\partial \tilde{\Lambda}} + \frac{\partial P_4}{\partial u_e}\right)\right] + \delta\left[\left(\frac{\mathrm{d}u_e}{\mathrm{d}x}\right)^2\frac{\partial P_5}{\partial u_e} - 2\frac{\mathrm{d}f}{\mathrm{d}x}\frac{\partial P_0}{\partial \tilde{\Lambda}} + P_5\frac{\mathrm{d}^2 u_e}{\mathrm{d}x^2} + \frac{3}{5}Ri\frac{\mathrm{d}Jx}{\mathrm{d}x}\right] - 2\frac{\partial P_0}{\partial u_e}\frac{\mathrm{d}u_e}{\mathrm{d}x}$$

with:

$$P_3 = P_2 + 2\frac{\partial P_2}{\partial \tilde{\Lambda}}, \qquad P_4 = 2\frac{\partial P_2}{\partial \tilde{\Lambda}}$$

$$P_5 = 2\left(P_1 + \frac{\partial P_2}{\partial u_e}\right)$$

References

[1] J.H. Merkin, Mixed convection from a horizontal circular cylinder, Internat. J. Heat Mass Trans. 20 (1977) 73–76.

[2] G.K. Sharma, S.P. Sukhatame, Combined free and forced convection heat transfer from a heated tube to a transverse air stream, J. Heat Trans. 91 (1969) 457–459.

[3] M. Amaouche, On some mixed convection flows described by exact solutions of Prandtl equations, European J. Mech. B Fluids 10 (1991) 295–312.

[4] D. Catherall, K.W. Mangler, The integration of two-dimensional laminar boundary layer equations past the point of vanishing skin-friction, J. Fluid Mech. 26 (1966) 163–175.

[5] F.J. Higuera, Opposite mixed convection flow in a wall jet over a horizontal plate, J. Fluid Mech. 342 (1997) 355–375.

[6] G. Polidori, M. Rebay, J. Padet, Retour sur les résultats de la théorie de la convection forcée laminaire établie en écoulement de couche limite externe 2D, Internat. J. Therm. Sci. 38 (1999) 398–409.